AN EXPERIMENTAL FACILITY FOR MEASURING THE ELECTRON ENERGY DISTRIBUTION FROM PHOTOCATHODES

L.B. Jones*, R.J. Cash, B.D. Fell, J.W. McKenzie, K.J. Middleman & B.L. Militsyn
STFC Daresbury Laboratory, ASTeC & the Cockcroft Institute, Warrington WA4 4AD, UK
H.E. Scheibler & A.S. Terekhov
Institute of Semiconductor Physics, SB–RAS, Novosibirsk 630090, Russia

Abstract

ASTeC has spent several years developing a GaAs Photocathode Preparation Facility (PPF) which routinely produces cathodes with quantum efficiencies (*Q.E.*) up to 20 % at 635 nm [1]. The goal is to use these and other cathode materials in high–average–current high–brightness injectors for particle accelerators.

Electron injector brightness is limited by source beam emittance, and brightness will be increased significantly by reducing the longitudinal and transverse energy spread in the emitted electrons, thereby creating a *cold beam.*

We are constructing an experimental system which is compatible with the PPF for measurement of the energy distribution in electrons emitted from photocathodes at room and LN_2-temperature. The photocathode will be illuminated by a small, variable–wavelength light spot. The electron beam image will be projected onto a detector comprised of a 3-grid energy filter, a microchannel plate and a phosphor screen. A low–noise CCD camera will capture screen images, and the spatial and energy distribution of the emitted electrons will be extracted through analysis of these images as a function of the grid potentials. The system will include a leak valve to progressively degrade the cathode, and thus allow its properties to be measured as a function of gas exposure.

INTRODUCTION

The ALICE[1] Energy Recovery Linac (ERL) utilises a DC electron gun, based on a Cs:GaAs photocathode. Currently, preparation of the cathode takes place *in–situ*, with the cathode first heat–cleaned, then activated prior to use by exposure to caesium and an oxidant (typically O_2 or NF_3) following established procedures [2, 3]. The PPF was designed as an upgrade to the ALICE photocathode gun to provide a superior environment for photocathode preparation, and to separate the activation process from the sensitive high–voltage environment.

Semiconductor Photocathode Properties

ALICE uses p^+-GaAs(100) in reflection mode as the photoemitter, highly–doped with Zn to a hole concentration level around $3 \pm 2 \times 10^{19}\,\mathrm{cm}^{-3}$. When activated, the vacuum level (E_{vac}) can fall *below* the bulk conduction band minimum level (E_c), creating the *negative electron affinity* (NEA) state. In an NEA material, electrons excited from the valence band into the conduction band have sufficient energy to escape into free space. Any excess energy (that above E_{vac}) translates into energy spread and hence emittance of the electron beam once in free space, whether the excess energy originates from the initial photon absorption process, or subsequent in–elastic scattering.

In a NEA semiconductor photocathode, energy spread is defined by the quantity $E_c - E_{vac}$. Unlike thermocathode electron sources, energy spread *increases* at low temperature because E_c increases [4]. By placing a bias on the photocathode source, it is possible to extract only those electrons whose energy exceeds the longitudinal energy barrier ($E_\parallel$) set by the bias, and when $E_\parallel \approx E_c$ the magnitude of the longitudinal and transverse energy spreads are close to the photocathode bulk temperature, kT [5]. The penalty when operating in this regime is the massive reduction in effective *Q.E.* by a factor of perhaps 30.

In principle, extracting electrons from a photocathode when $E_{vac} \approx E_c$ will also yield an electron beam with the lowest possible longitudinal and transverse energy spreads defined by the temperature of the photocathode itself. This equates to $kT = 7$ meV and 26 meV for photocathode temperatures of 77 K and 300 K respectively. Controlling E_{vac} in this way reduces energy spread in the emitted beam at the expense of photocurrent, thus reducing effective *Q.E.* but not to the same extent as when the source is biassed. This constitutes a mechanism to reduce energy spread, as is shown in Fig. 1.

Q.E. & Longitudinal Energy Spread

Fig. 1 shows the results of preliminary experiments carried out at the Institute of Semiconductor Physics in Novosibirsk. A photocathode activated to the NEA state was exposed to oxygen at a partial pressure of $\approx 7 \times 10^{-11}$ mbar, and measurements taken of photocurrent energy spectra as a function of anode collector voltage (*U*). The data shows that for fixed wavelength illumination, longitudinal energy spread $E_\parallel$ falls progressively as the oxygen exposure in Langmuirs (L) increases (i.e., energy spread decreases as *Q.E.* falls), and that the effect is more pronounced for photocathode illumination at 808 nm.

* lee.jones@stfc.ac.uk
[1] Accelerators and Lasers In Combined Experiments

ISBN 978-3-95450-115-1

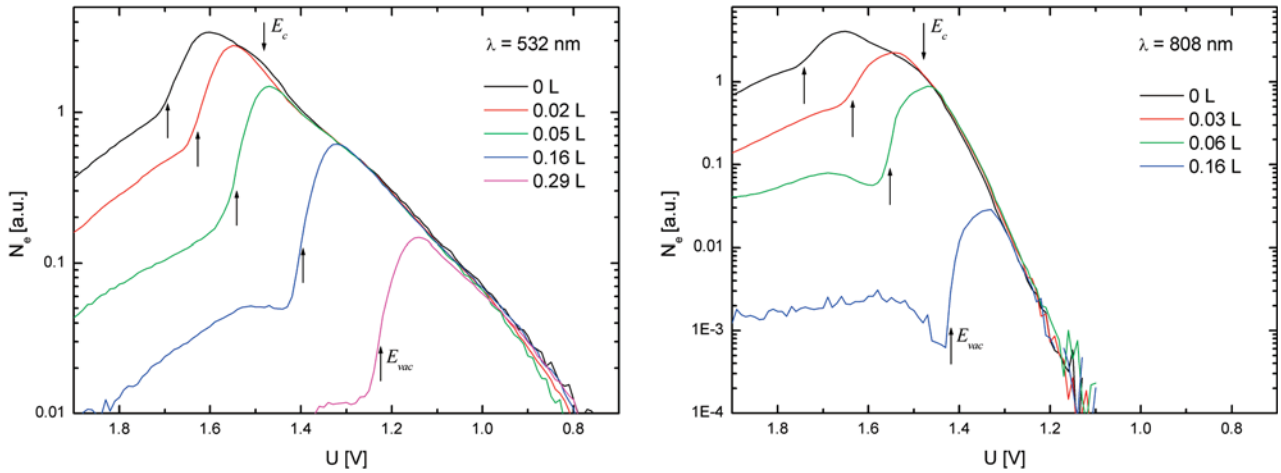

Figure 1: Experimental data showing how the vacuum level (E_{vac}) shifts and the number of emitted electrons (N_e) falls on increasing exposure to oxygen in Langmuir units (L) where 1 L exposure equates to a gas dose of 1×10^{-6} mbar·s. This leads to a progressive reduction in longitudinal energy spread as photocathode *Q.E.* falls. The **left** figure shows the photocathode response for illumination at 532 nm, and the **right** figure for illumination at 808 nm.

Photocathode degradation therefore reduces beam energy spread, and provides a mechanism to establish an ultracold beam from a semiconductor photocathode source.

EXPERIMENTAL DESIGN TO MEASURE 2-D ELECTRON ENERGY DISTRIBUTION

The results in Fig. 1 show that energy spread can be reduced by carefully controlling the vacuum level, E_{vac}. This is of interest to the particle accelerator community as it may lead to an increase in source beam brightness. We aim to study the transverse energy distribution ($E_\perp$) as a function of photocathode degradation, as $E_\perp$ essentially defines beam emittance.

The experimental system currently under construction will combine a vacuum chamber containing the photocathode mount and electron detector with the PPF, initially allowing the testing of semiconductor photocathodes prepared in a variety of different ways. The photocathode mount will incorporate cryogenic cooling, and FEA simulation has shown that the cathode surface will reach 77 K around 30 minutes after the reservoir is filled with LN_2. The mount will be electrically–isolated, so will support the application of a DC bias, and permit total–yield photocurrent to be measured. All materials used are both XHV–compatible and non–magnetic, and a mu-metal shield is included to screen the experimental region from the Earth's and other stray magnetic fields. See Figs. 2 and 3.

The vacuum vessel includes a piezo–electric leak valve which will allow controlled, continuous degradation of the photocathode *Q.E.* through over–oxidation. A cathode activated initially to a high NEA state can be studied over a period of time while its *Q.E.* is progressively lowered.

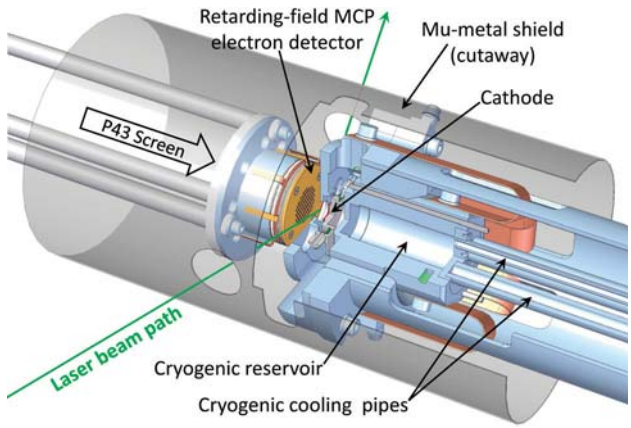

Figure 2: Detail view of the photocathode in the cryo–cooled mount and retarding–field electron detector.

Light Source

Photocathodes will be illuminated in reflection mode approximately 71° from the surface normal. Experiments will be carried out at fixed–wavelengths using 532, 635, 670, 780 and 808 nm diode lasers, with an option to use a broadband white light source and monochromator for spectral scanning in the range 200 to 950 nm. Access to UV wavelengths means that metal photocathodes can also be studied with this system. The optical layout will provide focussing to sub-100 μm spot size on the photocathode, and includes a photodiode to monitor laser power and hence *Q.E.*

Electron Detector

The detector is being manufactured by Hamamatsu, and combines a series of three retarding grids with a microchannel plate (MCP) and a P43 phosphor screen. Fig. 4 shows an exploded schematic of the detector assembly.

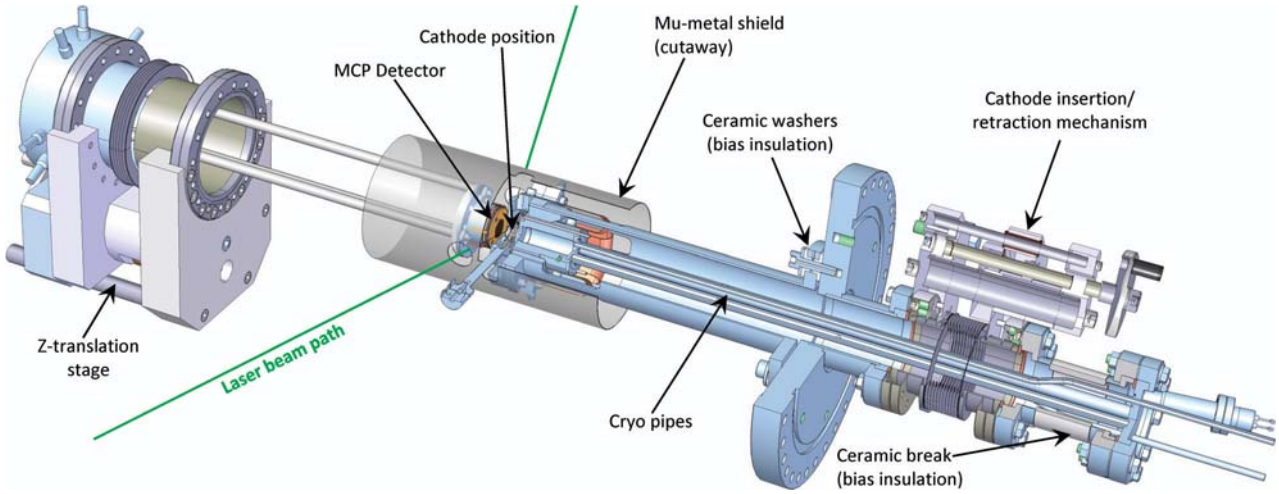

Figure 3: Schematic overview of the planned experimental system for measuring transverse energy spread. The vacuum vessel is removed for clarity, and the mu–metal shield and support stem are cut–away to show internal detail.

The grids will be gold–coated tungsten, manufactured by photo–etching to create high–conductivity, non–magnetic strands 5 μm wide on a 500 μm mesh–spacing. They will remain electrically isolated from each other at potentials up to 1 kV. The MCP is a 2-stage Hamamatsu model F1094 with an active area 20 mm ϕ which provides a gain approaching 10^7 at the maximum 2 kV bias level. The phosphor screen can operate at a maximum voltage of 6 kV, with the difference between itself and the MCP limited to 4 kV.

The detector assembly is mounted on a Z–translation stage which allows the distance between the photocathode source and the front grid to be varied from around 7.5 mm to 50 mm. This will permit data to be recorded with differing flight times, so highlighting the effects of transverse energy spread, and allowing accurate measurements of the transverse energy spread by selecting the distance which yields the highest fill level of the MCP active area.

Initial detector simulations were carried out in support of the instrument design using SIMION, and later a more sophisticated code in MatLab. Development of the MatLab model will continue to provide a set of optimised operating potentials, and ultimately to aid data analysis.

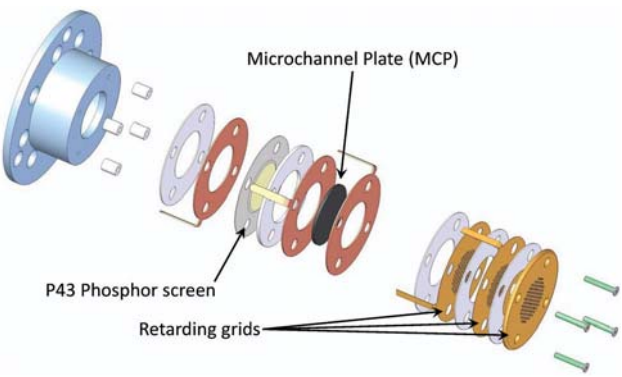

Figure 4: Schematic showing the 3-grid retarding–field electron detector with MCP electron–multiplier and P43 phosphor readout screen.

Data Acquisition Camera

Data will be collected using a low–noise, high–sensitivity PCO 2000 camera. The camera has a quantum efficiency around 50 % at the 543 nm emission wavelength of the phosphor screen. It is thermo–electrically cooled to -20 °C which yields a dark count rate of 0.01 e^-/pixel/s, and achieves a dynamic range of 4,400:1 from its 14 bit ADC. The square form factor of the 2048 × 2048 CCD array is ideally-suited for imaging the MCP output.

By scanning the potential applied to the retarding grids over a pre–defined range, a series of images will be taken which show the evolution of the transverse beam profile as a function of retarding voltage. Data will also be taken as a function of flight time by varying the photocathode–detector spacing. Analysis of the electron distribution in these images will yield the transverse energy, supporting photocathode optimisation work to achieve minimal transverse energy spread, and thus maximise beam brightness.

ACKNOWLEDGMENT

The authors would like to thank Dr. Oleg Karamyshev (University of Liverpool and the Cockcroft Institute) for initial modelling the retarding–field electron detector.

REFERENCES

[1] L.B. Jones, R.J. Cash, N. Chanlek, B.D. Fell, J.W. McKenzie, K.J. Middleman & B.L. Militsyn; Proc. IPAC '11, 3185-87.

[2] W.E. Spicer & R.L. Bell, Pub. Astron. Soc. **84** 110 (1972).

[3] W.E. Spicer, Appl. Phys. **12**, 115 (1977).

[4] A.S. Terekhov & D.A. Orlov, JETP Lett. **59** 864 (1994).

[5] D.A. Orlov, U. Weigel, D. Schwalm, A.S. Terekhov & A. Wolf, NIM 'A' **532** 418-421 (2004).

ISBN 978-3-95450-115-1